Journal of The Electrochemical Society, **158** (3) K64-K68 (2011)
0013-4651/2011/158(3)/K64/5/$28.00 © The Electrochemical Society

Field Emission and Magnetic Properties of Free-Standing Gd Silicide Nanowires Prepared by Reacting Ultrahigh Vacuum Deposited Gd Films with Well-Aligned Si Nanowires

Li-Wei Chu,[a,*] Shih-Wei Hung,[a,*] Chiu Yen Wang,[a,*] Yi-Hsin Chen,[a] Jianshi Tang,[b] Kang L. Wang,[b,] and Lih-Juann Chen[a,**,z]**

[a]*Department of Materials Science and Engineering, National Tsing Hua University, Hsinchu, Taiwan*
[b]*Device Research Laboratory, Department of Electrical Engineering, University of California, Los Angeles, California 90095, USA*

The well-aligned gadolinium silicide ($GdSi_{1.7}$) nanowire arrays were prepared by reacting ultrahigh vacuum deposited Gd with silicon nanowire arrays. The diameter of nanowires is 100 nm in average and lengths, thereof, were about several micrometers. Field emission measurement showed that the turn-on field of gadolinium silicide nanowires is as low as 0.75 V/μm at a current density of 10 μA/cm^2. The current density of 1 mA/cm^2 can be reached at an applied field of 2.1 V/μm. The field enhancement factor was determined to be 1222. Furthermore, the arrayed nanowires exhibit the ferromagnetic property at room temperature, which is attributed to magnetically uncompensated Gd atoms.
 [DOI: 10.1149/1.3529943]

Manuscript submitted May 24, 2010; revised manuscript received November 22, 2010. Published January 3, 2011.

Because the discovery of a number of superior physical properties for carbon nanotubes,[1] one dimensional (1-D) nanomaterials have drawn much attention for their potential applications.[2-4] In particular, metal silicide nanowires (NWs) have attracted much interest for use in the future electronic and magnetic devices.[5,6] Many silicides possess advantages such as low resistivity, good thermal stability, and low contact resistance with Si, which are promising candidates for improving the device performance and for the applications in optical communications, infrared detection, and displays.[7-9]

The rare-earth metal silicides have been widely studied for several decades due to its extremely low Schottky barrier height (0.3 eV)[10,11] on n-type silicon. As a result, rare-earth silicides form nearly Ohmic contact with silicon and have great potential as contacts and interconnections. A number of rare-earth silicides were reported in the forms of thin film and nanostructures. In particular, self-assembled rare-earth silicide NWs are easily obtained with high aspect ratio due to their unique lattice mismatch with Si.[12,13] One of the rare-earth silicides, gadolinium (Gd) silicide, has been reported to grow in the form of stable epitaxial thin film on silicon.[14,15] Excellent electrical properties and unique magnetic characteristics were disclosed.[16,17] On the other hand, the metal silicide film and molybdenum Spindt-type arrays have great field emission properties,[18-20] which were attributed to the low work function, high conductivity, and good thermal stability. Recently, metal silicide nanostructures exhibit superior field emission property due to the mechanical stability, large aspect ratio, and unique surface effect. This excellent property makes metal silicide nanostructures possess potential as field emitters.[21-25]

Furthermore, the magnetic properties of non-ferromagnetic materials in nano form have attracted a great deal of interests due to their distinct characteristics from the bulk materials. For example, ferromagnetism was observed in NiO nanoparticles (NPs) and in Co_3O_4 nanowires, both possessed antiferromagnetic properties in bulk.[26,27] Due to the large surface-to-volume ratio and the enormous number of uncompensated surface atoms, the magnetic properties were changed considerably in these NPs and NWs. In a previous study, thin films and bulk $GdSi_{1.7}$ were found to exhibit antiferromagnetic property with T_N = 40–55 K (Ref. 28) but Gd has ferromagnetism with T_C = 293 K. The magnetic properties of the arrayed nanowires were also discussed in this paper.

In anticipation of the properties of Ohmic contact on Si and favorable electron transport, the freestanding gadolinium silicides nanowires were grown by reacting ultrahigh vacuum (UHV) deposited Gd film deposited on silicon nanowire arrays. The gadolinium silicide nanowires exhibit superior properties of low turn-on field, high emission current density, and compatibility to microelectronic process. Moreover, ferromagnetic properties are observed at room temperature.

Experimental

The silicon nanowire arrays were prepared by electroless metal deposition and etching. The Si wafers were rinsed with acetone and ethanol in an ultrasonic bath for 15 min each consecutively. After rinsing with de-ionized water for several times, the Si wafers were dipped in a dilute HF solution for 1 min, followed by the final rinse in de-ionized water. The Si wafers were dispersed with 20 mM $AgNO_3$ solution and heated at 55°C for 20–60 min to undergo the etching process. The composition of etching solution is 0.07 g $AgNO_3$, 2 mL HF and 10 mL H_2O. At the end of etching, the silver particles were removed with dilute HNO_3 solution.[29,30]

After silicon nanowire arrays were obtained, the samples were introduced into a UHV chamber with a base pressure below 3 × 10^{-11} mbar, followed by degassing at ~700°C for at least 12 h. Gd (99.99% purity) evaporation was performed with a well-outgassed electron-beam evaporator at room temperature. The deposition rate was as low as 2 nm/min in a vacuum better than 1 × 10^{-9} mbar during the evaporation. The thickness of Gd layer ranged from 100 to 400 nm. Then the samples were annealed at 450–700°C by direct heating and the annealing time was from 2 to 6 h.

The synthesized samples were investigated with a JEOL 6500F field-emission scanning electron microscope (FESEM) and a JEM-3000F field-emission transmission electron microscope (FETEM) for morphology examination and phase identification. The X-ray diffraction (XRD) spectrum was obtained by MAC MXP-18 (40 kV, 200 mA, CuKa radiation). The wavelength is 1.54056 nm. The chemical compositions of nanowires were determined with an energy dispersive spectrometer (EDS) attached to the JEM-3000F TEM. The field emission properties of $GdSi_{1.7}$ nanowires were obtained in a KEITHLY model 237 system with the geometry of the parallel plates with a spacing of 200 μm at a pressure of 3 × 10^{-6} Torr. The magnetic properties of $GdSi_{1.7}$ NWs were determined using a superconducting quantum interference device (SQUID) magnetometer.

Results and Discussion

A high density array of silicon nanowires was obtained by electroless etching. According to the energy-dispersive X-ray analysis

* Electrochemical Society Student Member.
** Electrochemical Society Active Member.
z E-mail: ljchen@mx.nthu.edu.tw

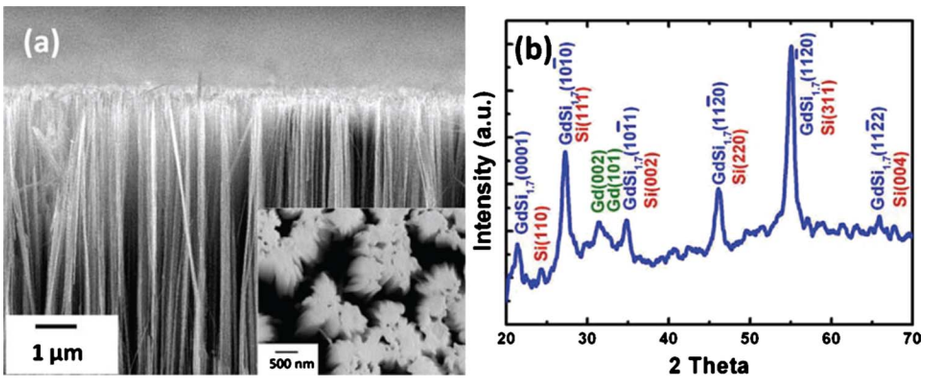

Figure 1. (Color online) (a) The FESEM image of arrayed $GdSi_{1.7}$ nanowires. Inset is the high-magnification SEM image. (b) The XRD spectrum of $GdSi_{1.7}$ nanowires.

(EDX) spectrum performed on whole sample, the Ag particles, the catalysts in electroless etching, were completely removed. Figure 1a shows the SEM image of nanowires annealed at 600°C for 6 h of Gd deposited nanowires. The morphology of nanowires hardly shows difference after deposition. The diameter and length of nanowires are 100 nm in average and up to 5 μm, respectively. The X-ray diffraction spectrum peaks can all be ascribed exactly to hexagonal GdSi1.7, Gd and Si, as shown in Fig. 1b.

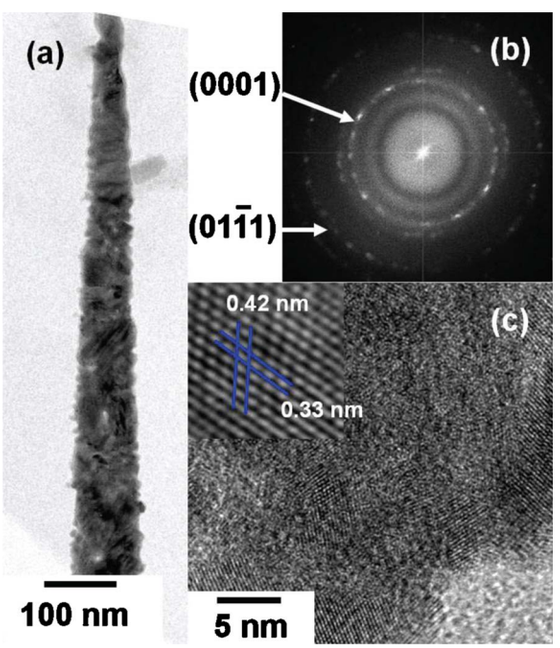

Figure 2. (Color online) (a) TEM image of a $GdSi_{1.7}$ nanowire after 6 h annealing, (b) diffraction pattern of the polycrystalline $GdSi_{1.7}$ nanowires, and (c) The high resolution image shows many fine grains and inset shows the spacing consistent with $GdSi_{1.7}$.

The TEM image of a nanowire after 6 h of annealing is shown in Fig. 2a. The nanowire is about 90 nm in diameter. Figure 2b is a selected area electron diffraction (SAED) pattern revealing that the hexagonal phase $GdSi_{1.7}$ is polycrystalline. The high resolution image, shown in Fig. 2c, discloses the lattice spacings consistent with those of hexagonal $GdSi_{1.7}$ phase. In addition, Fig. 2c shows clearly the fine grains in the polycrystalline $GdSi_{1.7}$ nanowires. The grains are 3 nm in average size. From the mapping and EDS spectrum, shown in Fig. 3, both Si and Gd were detected and dispersed uniformly in the body but Gd formed segregation at the top of the nanowire. The ratio of Si and Gd in the body of nanowires are close to 1.7, so that the composition also verifies the phase of $GdSi_{1.7}$, the defective Gd disilicide. Furthermore, the ratio of the composition is the same for tens of nanowires analyzed.

The growth of freestanding $GdSi_{1.7}$ nanowires was difficult because rare-earth elements are known to be easily oxidized. Due to the high reactivity with oxygen, the formation of rare-earth silicides requires either ultra high vacuum or protective capping layer to prevent them from oxidation.[31] Only under UHV deposition and annealing to react the Gd film with Si nanowires, freestanding Gd nanowires were formed. A further advantage in using well-aligned Si nanowires as the templates is that the dimensions of nanowires could be facilely controlled by the electroless etching process.

The field emission properties were measured in parallel plate geometry with a spacing of 200 μm at a pressure of 3×10^{-6} Torr. The contact area was 0.09 cm^2. The emission current was recorded as the applying voltage increasing with a step of 5 V at a time. The current density as a function of the applied field of the $GdSi_{1.7}$ nanowires after 6 h of annealing is shown in Fig. 4. The turn-on field of the nanowires was found to be 0.75 V/μm with the current density reaching 10 $\mu A/cm^2$. The field emission current density is as high as 1 mA/cm^2 at an electric field of 2.1 V/μm. The

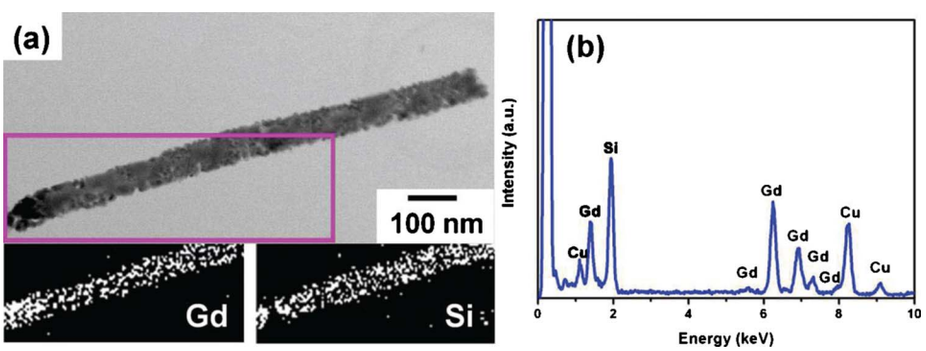

Figure 3. (Color online) (a) The images of elemental mapping of Gd and Si. (b) The TEM/EDS spectrum.

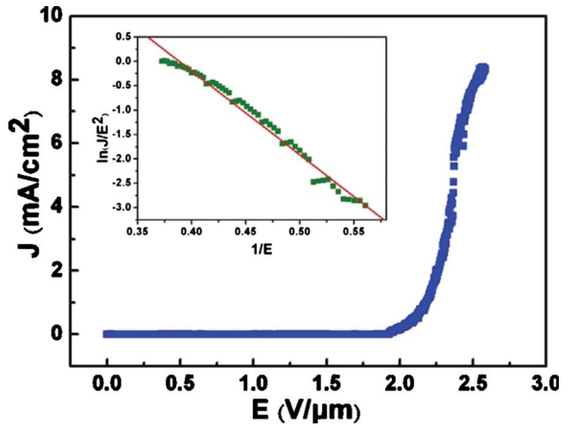

Figure 4. (Color online) J-E curve of field emission characteristic of the $GdSi_{1.7}$ nanowires after 6 h of annealing. The inset is the FN plot of the emission of nanowires.

$\ln(J/E^2) - 1/E$ plot in the inset of Fig. 4 shows a straight line, which indicates that it follows Fowler–Nordheim (FN) behavior. The Fowler–Nordheim equation is

$$J = (A\beta^2E^2/\Phi)\exp(-B\Phi^{3/2}/\beta E) \quad [1]$$

where J is the current density, E is the applied electric field, Φ is the work function of the emission material, and β is the field enhancement factor. A and B are constants, corresponding to 1.56×10^{-10} (A V^{-2} eV) and 6.83×10^3 (V $eV^{-3/2}$ μm^{-1}), respectively. The emission properties were dominated by the emission material and the field enhancement factor. The work function is an intrinsic property of material. The field enhancement factor was generally determined by the crystal structure, surface morphology, and effective emission sites. The work functions of three stoichiometric types of silicides were reported to be 3.05, 3.7, and 4.1 eV for Gd-rich silicide, monosilicide, and Si-rich silicide, respectively.[32,33] Utilizing the FN equation and applying the work function of Si-rich silicide (Φ = 4.1 eV), the field enhancement factor β was calculated to be 1222. The β value is higher than thin film structure of gadolinium silicides[20] and comparable to many other 1-D nanowires of interest, such as $TiSi_2$ (β = 500), $NiSi_2$ (β = 630), Ti_5Si_3 (β = 816), Si (β = 1000), and $TaSi_2$ (β = 1200–1800).[21-25] The low turn-on field also compares favorably with other nanostructures, such as Si nanocone (16.5 V/μm).[24] Ni_2Si nanowires (3.4 V/μm),[9] $TaSi_2$ nanowires (5.3 V/μm),[25] and CoSi (1.42 V/μm).[34] Furthermore, these field emission characteristics are significantly superior than those of silicon nanowires.[35,36] In addition, the current density was high and stable even over the threshold field. The excellent field emission properties are attributed to the low Schottky barrier height with silicon substrates. This characteristic enhanced the electrons transporting from the silicon substrates to the silicide nanowire surfaces and improved the field emission performance.

The stability of field emission was also apparent in repeated measurements as shown in Fig. 5a. The field emission characteristics are reversible and reproducible. In addition, all the measurements were checked with the leakage current. The leakage current was measured by reversing the electrodes. However, there was no observable current obtained even at the highest applied field. The $GdSi_{1.7}$ nanowires can be concluded to have the excellent field emission characteristics.

The superb field emission characteristics of high current density are attributed to low work function of $GdSi_{1.7}$ as well as minimal screening effect.[37] The work function of $GdSi_{1.7}$ is lower than other silicides, such as $NiSi_2$ (4.7 eV)[7] and $TiSi_2$ (4.6 eV).[21] On the other hand, the top-view SEM of $GdSi_{1.7}$ nanowires is shown in the inset of Fig. 1a. The nanowires form bundles and the inter-distance ranges from 400 nm to 1.5 μm. Because the length of metal silicide part is around 600 nm observed in the TEM images, the interwire distance and the length of silicide part match the ratio by 1–2 to alleviate the screening effect.[38] The screening effect arose from dense emission sites, which caused the local electric field to be compensated by interference abruptly. In the present work, the density of nanowires was selected to alleviate screening effect resulting in very high current density.

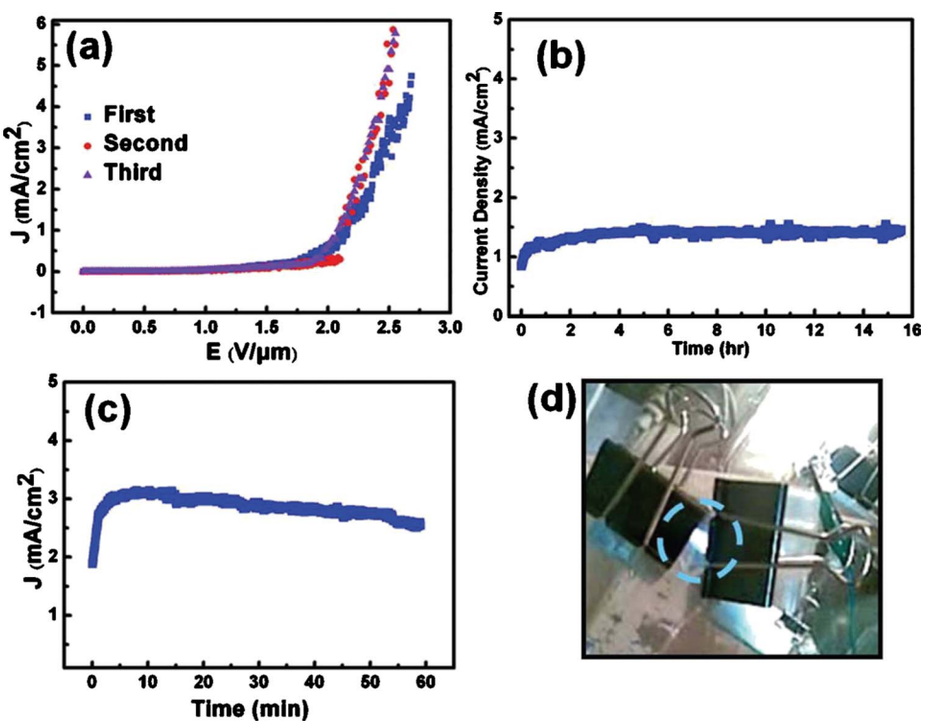

Figure 5. (Color online) (a) J-E curves obtained from three consecutive measurements. (b) The stress test under fixed electric field of 2.1 V/μm over 15 h. (c) A similar stress test under fixed electric field of 2.3 V/μm. (d) Field emission image from the $GdSi_{1.7}$ nanowires.

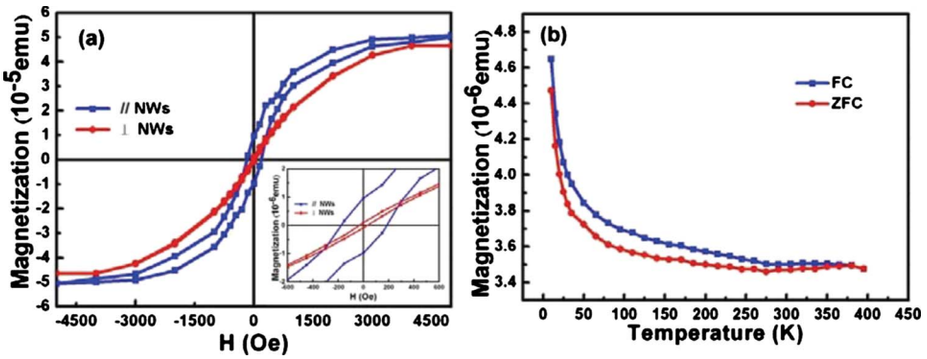

Figure 6. (Color online) (a) The room-temperature SQUID hysteresis loops of arrayed nanowires, (b) ZFC and FC magnetization curves as a function of temperature.

The high current density and low turn-on voltage are advantageous for the various applications, such as cold cathode emitter and flat plate display. For these applications, the stability test is necessary to ensure the operation of the product. As a result, the stress tests were carried out under a fixed applied field for a long period of time and the variations of current were recorded with elapsed time. The stress tests shown in Figs. 5b and 5c were constructed under applied fields of 2.1 and 2.3 V/μm, which led to the average current densities of 1.37 and 2.86 mA/cm^2, respectively. It was found that the current density under the applied field of 2.1 V/μm was barely degraded over 15 h measurements. On the other hand, the current density under the applied field of 2.3 V/μm was degraded for about 15% within 1 h measurement. The higher applied field induces higher current density and inflicts more severe damages on the nanowires. It was worth noting that at the beginning of the stress test, the current density was increased to 3 mA/cm^2. The phenomenon may be ascribed to desorption of atoms on the nanowires under the high electric field. In the present work, the $GdSi_{1.7}$ nanowires were proved to be stable for several hours with current density of 1 mA/cm^2, which is higher than the operation current density of flat panel display. Moreover, the current densities were essentially constant with several on/off circles. These characteristics could be beneficial for the applications in display or for other emitting devices.

In order to demonstrate the practical applicability of the $GdSi_{1.7}$ nanowires as field emitters, a simple field emission device was constructed. The upper anode was replaced by indium-tin oxide (ITO) coated with phosphor thin film. The composition of phosphor is Y_2O_2S:Tb. The whole device was also in a parallel plate geometry with a spacing of 200 μm and the contact area was 0.5 cm^2. Although the applied field was over the threshold field (2.1 V/μm), the device was lightened up brightly and uniformly as shown in Fig. 5d. The strong and uniform emission of $GdSi_{1.7}$ nanowire array is critically important for practical applications as field emitters.

Figure 6a shows two room-temperature SQUID hysteresis loops of the arrayed NWs when the external magnetic fields were applied parallel and perpendicular to the NWs. These two hysteresis loops indicated that the NWs possess ferromagnetism at room temperature and demonstrate the distinct anisotropic magnetic property. For the applied magnetic field parallel to the NWs, the hysteresis loop exhibits a hard magnetization axis with the coercive field of 180 Oe and high remanence. On the other hand, for the applied magnetic field perpendicular to the NWs the hysteresis loop shows an easy magnetization axis with the coercive field of 29 Oe and low remanence. In bulk materials, the same magnetic properties should be obtained whether the applied field was perpendicular or parallel to the substrate. The anisotropic magnetic characteristics for the arrayed NWs were similar to the various NWs disclosed in other works.[39,40] It was normally attributed to the non-identical magnetic coupling due to the anisotropic aspect ratio of the NWs.

$GdSi_{1.7}$ is an antiferromagnetic material in bulk with T_N = 40–55 K. Similar behavior was also observed in various antiferromagnetic or diamagnetic NPs or NWs.[27,41,42] Different models have been proposed to explain ferromagnetic property in nanoform, such as uncompensated spins on two sublattices and reduced coordination of the surface spins. However, the Curie temperature of Gd is 293 K disclosed in several literatures, Gd segregations are believed to contribute the magnetization at room temperature (300 K). The nano-scaled Gd clusters might provide uncompensated spins and contribute the magnetization beyond the T_C of Gd. Moreover, strain or structural defects in crystal might also induce ferromagnetism.[26,27] The magnetic property is therefore likely to be due to the reduced coordination of the Gd atoms in the NWs, in which surface spins are not fully compensated.

The zero-field-cooled (ZFC) and field-cooled (FC) magnetization in an applied magnetic field of 100 Oe curves were obtained as a function of temperature, as shown in Fig. 6b. The difference of ZFC and FC measurements is possible by applying magnetic field during the cooling process. The FC curve exhibits higher magnetization than ZFC curve at low temperature. This should be attributed to the extra spin order caused by the applied field. However, the spins disorder severely due to the thermal agitation at high temperature and the FC curve shows the same magnetization with ZFC curve. Moreover, the M-T curves showed room-temperature ferromagnetism characteristics as well.

Conclusions

In summary, freestanding $GdSi_{1.7}$ nanowires were prepared by reacting UHV deposited Gd film on silicon nanowire arrays. With the proper deposition rate and annealing time, the uniform polycrystalline $GdSi_{1.7}$ nanowires were obtained. The field emission measurements showed that the turn-on field of $GdSi_{1.7}$ nanowires is as low as 0.75 V/μm at a current density of 10 μA/cm^2. The current density of 1 mA/cm^2 can be reached at an applied field of 2.08 V/μm and the field enhancement factor reached 1222. The stability test of emission current density exhibited essentially no degradation at 1.37 mA/cm^2 over 15 h. The growth of $GdSi_{1.7}$ nanowires was made possible by combining the deposition of Gd on aligned and properly spaced Si nanowires and annealing in UHV. The low turn-on field and high current density are attributed to low work function of $GdSi_{1.7}$ and minimal screening effect of the nanowire arrays. The $GdSi_{1.7}$ nanowires with superb field emission characteristics are potentially useful as field emitters and cold cathodes applicable in flat panel displays. For the magnetic properties, the arrayed nanowires showed distinct behaviors compared to the bulk material. The room-temperature ferromagnetism is attributed to the uncompensated Gd atoms. The anisotropic magnetic properties were observed by changing the direction of the applied magnetic field.

Acknowledgment

The authors acknowledge the National Science Council, Taiwan (ROC) for support through grant no. NSC 98-2221-E-007-104-MY3.

National Tsing Hua University assisted in meeting the publication costs of this article.

References

1. S. Iijima, *Nature (London)*, **354**, 56 (1991).
2. Z. Yu and M. Aceves-Mijares, *Appl. Phys. Lett.*, **95**, 081101 (2009).
3. A. L. Schmitt, M. J. Bierman, D. Schmeisser, F. J. Himpsel, and S. Jin, *Nano Lett.*, **6**, 1617 (2006).
4. Q. Zhao, J. Xu, X. Y. Xu, Z. Wang, and D. P. Yu, *Appl. Phys. Lett.*, **85**, 5331 (2004).
5. W. M. Weber, L. Geelhaar, A. P. Graham, E. Unger, G. S. Duesgerg, A. Liebau, W. Pamler, C. Cheze, H. Riechert, P. Lugli, et al., *Nano Lett.*, **6**, 2660 (2006).
6. A. L. Schmitt, J. M. Higgins, and S. Jin, *Nano Lett.*, **8**, 810 (2008).
7. C. Y. Lee, M. P. Lu, K. F. Liao, W. F. Lee, C. T. Huang, S. Y. Chen, and L. J. Chen, *J. Phys. Chem. C*, **113**, 2286 (2009).
8. C. M. Chang, Y. C. Chang, C. Y. Lee, P. H. Yeh, W. F. Lee, and L. J. Chen, *J. Phys. Chem. C*, **113**, 9153 (2009).
9. L. J. Chen, *JOM*, **57**, 24 (2005).
10. P. L. Janega, J. McCaffrey, and D. Landheer, *Appl. Phys. Lett.*, **55**, 1415 (1989).
11. K. N. Tu, R. D. Thompson, and B. Y. Tsaur, *Appl. Phys. Lett.*, **38**, 626 (1981).
12. Z. He, D. J. Smith, and P. A. Bennett, *Appl. Phys. Lett.*, **86**, 143110 (2005).
13. W. Zhou, Y. Zhu, T. Ji, X. Hou, and Q. Cai, *Nanotechnology*, **17**, 852 (2006).
14. G. L. Molna, G. Peto, Z. Ve'rtesy, and E. Zsoldos, *Appl. Phys. Lett.*, **74**, 1672 (1999).
15. B. C. Harrison and J. J. Boland, *Surf. Sci.*, **594**, 93 (2005).
16. C. Pescher, J. Pierre, A. Ermolieff, and C. Vannuffel, *Thin Solid Films*, **278**, 140 (1996).
17. P. Majumdar and S. Kumar, *Phys. Rev. Lett.*, **90**, 237202 (2003).
18. N. G. Shang, F. Y. Meng, F. C. K. Au, Q. Li, C. S. Lee, B. Igor, and S. T. Lee, *Adv. Mater.*, **14**, 1308 (2002).
19. H. S. Uh and S. S. Park, *J. Electrochem. Soc.*, **150**, H12 (2003).
20. H. G. Duan, E. Q. Xie, and F. Ye, *J. Appl. Phys.*, **101**, 064503 (2007).
21. B. Xiang, Q. X. Wang, Z. Wang, X. Z. Zhang, L. Q. Liu, J. Xu, and D. P. Yu, *Appl. Phys. Lett.*, **86**, 243103 (2005).
22. Y. W. Ok, T. Y. Seong, C. J. Choi, and K. N. Tu, *Appl. Phys. Lett.*, **88**, 043106 (2006).
23. H. K. Lin, Y. F. Tzeng, C. H. Wang, N. H. Tai, I. N. Lin, C. Y. Lee, and H. T. Chiu, *Chem. Mater.*, **20**, 2429 (2008).
24. Y. L. Chueh, L. J. Chou, S. L. Cheng, J. H. He, W. W. Wu, and L. J. Chen, *Appl. Phys. Lett.*, **86**, 133112 (2005).
25. Y. L. Chueh, M. T. Ko, L. J. Chou, L. J. Chen, C. S. Wu, and C. D. Chen, *Nano Lett.*, **6**, 1637 (2006).
26. R. H. Kodama, S. A. Makhlouf, and A. E. Berkowitz, *Phys. Rev. Lett.*, **79**, 1393 (1997).
27. E. L. SalaBas, A. Rumpleker, F. Kleitz, F. Radu, and F. Schuth, *Nano Lett.*, **6**, 2977 (2006).
28. L. D. Tung, K. H. J. Buschow, J. J. M. Franse, and N. P. Thuy, *J. Magn. Magn. Mater.*, **154**, 96 (1996).
29. K. Peng, J. Hu, Y. Yan, Y. Wu, H. Fang, Y. Xu, S. T. Lee, and J. Zhu, *Adv. Funct. Mater.*, **16**, 387 (2006).
30. K. Peng, H. Fang, J. Hu, Y. Wu, J. Zhu, Y. Yan, and S. T. Lee, *Chem.-Eur. J.*, **12**, 7942 (2006).
31. J. C. Chen, G. H. Shen, and L. J. Chen, *J. Appl. Phys.*, **84**, 6083 (1998).
32. S. Lee, A. Shinde, and R. Ragan, *Nanotechnology*, **20**, 035701 (2009).
33. S. A. Shakirova and E. V. Serova, *Appl. Surf. Sci.*, **219**, 363 (2003).
34. C. I. Tsai, P. H. Yeh, C. Y. Wang, H. W. Wu, U. S. Chen, M. Y. Lu, W. W. Wu, L. J. Chen, and Z. L. Wang, *Cryst. Growth Des.*, **9**, 4514 (2009).
35. X. Fang, Y. Bando, C. Ye, G. Shen, U. K. Gautem, C. Tang, and D. Golberg, *Chem. Commun. (Cambridge)*, **2007**, 4093.
36. C. Li, G. Fang, S. Sheng, Z. Chen, J. Wang, S. Ma, and X. Zhao, *Physica E (Amsterdam)*, **30**, 169 (2005).
37. V. Filip, D. Nicolaescu, M. Tanemura, and F. Okuyama, *Ultramicroscopy*, **89**, 39 (2001).
38. L. Nilsson, O. Groening, C. Emmenegger, O. Kuettel, E. Schaller, L. Schlapbach, H. Kind, J.-M. Bonard, and K. Kern, *Appl. Phys. Lett.*, **16**, 2071 (2000).
39. Y. L. Chueh, L. J. Chou, J. Song, and Z. L. Wang, *Nanotechnology*, **18**, 145604 (2007).
40. J. Choi, S. J. Oh, H. Ju, and J. Cheon, *Nano Lett.*, **5**, 2179 (2005).
41. Y. Wang, C. M. Yang, W. Schmidt, B. Spliethoff, E. Bill, and F. Schuth, *Adv. Mater.*, **17**, 53 (2005).
42. L. Suber, D. Fiorani, G. Scavia, P. Imperatori, and W. R. Plunkett, *Chem. Mater.*, **19**, 1509 (2007).